Palaeogeography, Palaeoclimatology, Palaeoecology 659 (2025) 112672

Contents lists available at ScienceDirect

Palaeogeography, Palaeoclimatology, Palaeoecology

journal homepage: www.elsevier.com/locate/palaeo

Environmental changes in East-Central Europe from a Middle to Late Holocene Romanian cave sediment record

Bogdan P. Onac[a,b], Angelica Feurdean[c], Aritina Haliuc[b], Simon M. Hutchinson[d], Ferenc L. Forray[b,e], Andrea Demjén[f,b], Adriana Vulpoi[b], Răzvan Dumbravă[g,b], Adrienn Lőrincz[h], Călin Ghemiș[i,b], Augustin Nae[j], Viorel T. Lascu[k], Florin Gogâltan[l], Ioana N. Meleg[b,j,*]

[a] School of Geosciences, University of South Florida, 4202 E. Fowler Ave., Tampa 33620, USA
[b] Emil G. Racoviță Institute, Babeș-Bolyai University, Clinicilor 5-7, 400006 Cluj-Napoca, Romania
[c] Department of Physical Geography, Goethe University, Altenhöferallee 1, 60438 Frankfurt am Main, Germany
[d] School of Science, Engineering and Environment, University of Salford, Salford, Greater Manchester M5 4WT, UK
[e] Department of Geology, Babeș-Bolyai University, Kogălniceanu 1, 400084 Cluj-Napoca, Romania
[f] National Museum of Transylvanian History, C. Daicoviciu 2, 400020 Cluj-Napoca, Romania
[g] University of Oradea, Faculty of Geography, Tourism and Sport, Department of Geography, Tourism and Territorial Planning, University 1, 410087 Oradea, Romania
[h] University of Debrecen, Egyetem tér 1, 4032 Debrecen, Hungary
[i] Criș Country Museum, Calea Armatei Române 1A, 410087 Oradea, Romania
[j] Emil Racoviță Institute of Speleology of the Romanian Academy, Calea 13 Septembrie 13, Bucharest, Romania
[k] National Institute for Research and Development in Environmental Protection, 060031 Bucharest, Romania
[l] Institute of Archaeology and Art History, Kogălniceanu 12-14, 400084 Cluj-Napoca, Romania

ARTICLE INFO

Editor: P Hesse

Keywords:
Karst
^{14}C dating
Geochemistry
Multi-proxies
Charcoal
Romania

ABSTRACT

Caves are sensitive to hydrological processes including sediment transport associated with changes in external climatic conditions. When located in the proximity of prehistoric settlements, cave sediments can provide details about human activities and help to elucidate the paleoenvironment. Here, we present a comprehensive analysis of lithological, geochemical, magnetic, organic matter, non-pollen palynomorphs, and charcoal data from sediment in Ciur Izbuc Cave, revealing significant paleoenvironmental and hydrodynamic changes over the past 6500 years. The first phase (6500–3500 calibrated years BP; cal BP) depicts a dynamic system with constant surface-subsurface connections, moderate-to-high erosion, and low-to-moderate sediment accumulation rates. The low charcoal levels during this phase indicate limited human impact. The second phase (3500–1400 cal BP) features contrasting depositional environments; the initial interval shows low accumulation under reduced water flow, reflective of a stable late mid-Holocene climate, while the subsequent interval reveals an abrupt shift to wetter conditions, characterized by runoff-derived minerogenic sediments. This period coincides with increased human impacts, including fire activity and land-use changes since the late Bronze Age. The third phase (1400–100 cal BP) exhibits complex hydrological dynamics, with sporadic, intense erosion linked to short-term climatic shifts. Increased charcoal concentrations and the presence of fungi indicate persistent human activity, intensifying after 300 cal BP. Our findings underscore the complex relationship between climate events, humans, and sediment dynamics in the Ciur Izbuc Cave, highlighting the utility of a multi-proxy approach in reconstructing past environmental changes.

1. Introduction

Cave sediments are unique archives of past environmental change with an exceptional scientific value. Trapped within caves, these sediments can serve as important records capturing changes that occur in the surrounding environment over hundreds of thousands of years (Osborne, 1986; White, 2007; McAdams et al., 2019). Cave development and the accumulation of sediments are related to their geomorphic

* Corresponding author at: Emil G. Racoviță Institute, Babeș-Bolyai University, Clinicilor 5-7, 400006 Cluj-Napoca, Romania.
E-mail address: ioana.meleg@ubbcluj.ro (I.N. Meleg).

https://doi.org/10.1016/j.palaeo.2024.112672
Received 5 June 2024; Received in revised form 31 October 2024; Accepted 14 December 2024
Available online 16 December 2024
0031-0182/© 2024 The Authors. Published by Elsevier B.V. This is an open access article under the CC BY-NC-ND license (http://creativecommons.org/licenses/by-nc-nd/4.0/).

evolution, and thus, processes operating at the surface (e.g., floods, variations in the water table, etc.) directly impact the sedimentation inside the cave. Erosional, transport and depositional processes vary with time and with changes in external regional scale factors, such as climate, tectonic activity, and surface geomorphology, ultimately providing a comprehensive integration of broader landscape evolution (Sasowsky and Mylroie, 2004; Farrant and Smart, 2011; Arriolabengoa et al., 2015). However, compared to surface records, cave sediment sequences are poorly documented and more challenging to interpret because their deposition is heterogeneous and discontinuous with temporal gaps leading to complex stratigraphic results, which can preclude detailed paleoenvironmental interpretation (Plotnick et al., 2015; Gillieson, 2021). Sometimes, several sequences are needed to obtain a complete and continuous record. In such depositional environments, it is crucial to establish precise chronologies and understand the erosional events to elucidate the relationship between surface and underground processes (White, 2007).

Despite the recent advances in this field and an increase in the number of publications focused on natural records, regions like East-Central Europe (hereafter ECE) still exhibit a deficit in cave sediment research (Gillieson, 2021). Caves are often key archaeological sites and are known to preserve a plethora of long-term and critical information related to human evolution. They have served as shelters for humans, often serving as focal points for paleontological and archaeological research. Therefore, sedimentary studies play a vital role in offering information about the environmental and climatic conditions that humans lived in or how the cave environments were used (Hunt et al., 2015).

In the Romanian Carpathians, previous work from cave environments focused on speleothems (Onac et al., 2002; Drăgușin et al., 2014; Warken et al., 2018), bat guano (Onac et al., 2014; Forray et al., 2015; Cleary et al., 2018) and ice (Feurdean et al., 2011; Perșoiu et al., 2017; Bădăluţă et al., 2020) to reconstruct past climate variability and environmental changes over the past millennia. However, multi-proxy based approaches (trace elements, carbon and nitrogen isotopes, testate amoebae, plant macrofossils, charcoal, pollen) from other archives including lake, peat-bogs, (Feurdean et al., 2008; Magyari et al., 2009; Diaconu et al., 2017; Longman et al., 2019; Ramos-Román et al., 2022), fluvial records (Chiriloaei et al., 2012; Perșoiu and Perșoiu, 2018), tree rings (Popa and Kern, 2009; Nagavciuc et al., 2022), cave sediments (Moldovan et al., 2016), and documentary sources (Perșoiu and Perșoiu, 2018) have also been used in this region to unveil changes in its climate and environment over the past several millennia.

The region (ECE) lies at the intersection of three different climatic

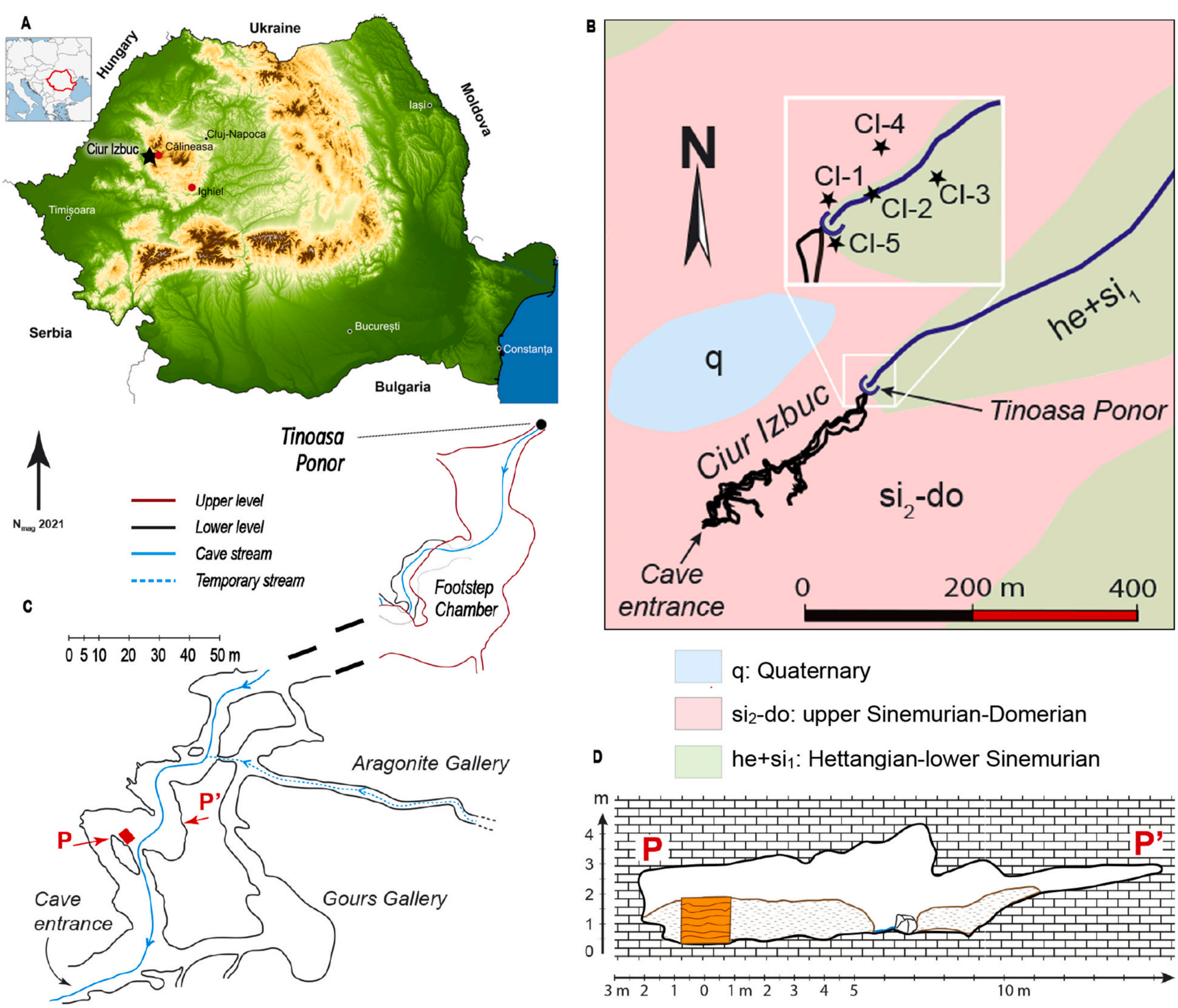

Fig. 1. A). Location of Ciur Izbuc Cave in northwestern Romania (black star). B) Geological map of the cave area, with the inset showing surface soil sampling sites (based on data from Bădescu, 1986). C). Cave map showing only the lower and upper sections, with a dashed line indicating the missing portion. The sediment sequence location near the cave entrance is marked by a red rectangle). D) Cross-section of the cave gallery, showing the alluvial deposits and the investigated profile (orange). (For interpretation of the references to colour in this figure legend, the reader is referred to the web version of this article.)

systems: Atlantic, Continental, and Mediterranean (Busuioc et al., 2015) and is regarded as a westward corridor for modern human dispersal since at least 43,000 years ago (Chu, 2018). The area has a rich history of human habitation dating back to the early Neolithic period (Raczky, 2014). The earliest evidence of human presence in the Pădurea Craiului Mountains (northwestern Romania; Fig. 1a), our study area, has been identified in Ciur Izbuc Cave and dates to a period between 36,500 and 28,700 cal BP (Webb et al., 2014). Additionally, Upper Paleolithic rock paintings in Coliboaia Cave, located nearby, have been attributed to this period (Clottes et al., 2013). Towards the end of the Middle Neolithic (~7000 cal BP), small human communities used caves in the region as shelter and ritual spaces (Ghemiș, 2021; Savu and Gogâltan, 2021; Gogâltan et al., 2023). A notable increase in habitation occurred at the onset of the Copper Age period (~6500 cal BP), marked by the interest of Tiszapolgár communities in exploring copper and gold deposits slightly more distant from our study area. Thus, the study cave and its surroundings could be key to understanding past environmental changes and elucidating their relationship with human presence.

Here we contribute to this line of research by conducting a multi-proxy investigation (geochemical and mineralogical data, grain-size analysis, mineral and organic content, mineral magnetic information, charcoal, and non-pollen palynomorphs) of a 128-cm-long excavated sediment outcrop in Ciur Izbuc Cave, spanning the last 6500 years. Our primary objectives are: *i)* To identify the main depositional processes inferred from the sedimentary sequence and to understand how these processes shed light on past environmental and climatic changes and *ii)* To assess in what ways the reconstruction of climatic, hydrological, and vegetation changes, derived from cave sedimentary proxies compare with other (hydro)climate and local/regional vegetation shifts documented elsewhere in Romania.

2. Regional setting

Ciur Izbuc Cave (N 46°51′10″, E 22°24′00″) is located in the south-eastern part of the Pădurea Craiului Mountains in northwestern Romania (Fig. 1A). The region exhibits a diverse geological makeup (Ianovici et al., 1976) and is renowned for its karst landscapes, which encompass underground drainage systems, caves and sinkholes (Rusu, 1988). The climate in the area is identified as a wet temperate continental subtype (Dfb in the Köppen climate classification). Local weather monitoring near the cave from 2019 to 2021 shows temperatures ranging between −6.8 and 14.5 °C (average − 1.7 °C) during the cold season and between 10.28 and 28.44 °C (average 23.6 °C) in the summer (Borda et al., 2022). Precipitation levels indicate moderate rainfall throughout the year, with the highest recorded during winter 2021 (3.74 mm/day) and the lowest during winter 2020 (0.71 mm/day).

The Runcuri Karst Plateau has a surface area of 7 km^2 and a median elevation of 500 m above sea level. The vegetation is predominantly composed of beech (*Fagus sylvatica*) forest. Additionally, *Cynosurion cristati* grasslands are present in the area (Groza, 2008).

Ciur Izbuc Cave is formed in a Lower Jurassic (Upper Sinemurian-Pliensbachian; Fig. 1B) carbonate unit (Bădescu, 1986) and consists of an upper fossil level and a lower level, with a 425 m-long underground ephemeral stream. The upper level holds a remarkable discovery made during exploration of the cave in 1965: the Footstep Chamber, where approximately 400 human footprints were imprinted in reddish-brown clay (Rusu et al., 1969). A study conducted by Webb et al. (2014) focused on 51 footprints and radiocarbon dated cave bear bones as indirect evidence to estimate the age of the human footprints. Their findings suggest that people could have inhabited Ciur Izbuc Cave at various times since ~36,500 years ago.

The lower level of the cave is drained by a stream that disappears underground through the Tinoasa Ponor, located just 20 m from the upstream end of the cave (Fig. 1B). This level originated during the Upper Pleistocene and Holocene, when erosional notches and alluvial terraces formed within the cave, reflecting fluctuations in water discharge (Rusu, 1988). As the water table drops, the underground stream adjusts by incising downward, progressively exposing alluvial sediments accumulated over millennia.

3. Materials and methods

3.1. Lithology and chronology

The sampled sediment sequence is located 30 m from the cave entrance (Fig. 1C, D). To expose the full sediment profile, we opened a test trench (150 × 220 × 128 cm) that, once carefully cleaned, provided a vertical sedimentary profile of 128 cm. After removing the oxidative layer to avoid possible contamination, we collected 64 sediment samples at 2 cm resolution. Each sample was sealed in plastic zip bags and stored at 4 °C. Geochemical composition, magnetic properties, loss-on-ignition, carbon and nitrogen content and particle size of 64 samples were analyzed at the University of Salford (UK). A pre-analysis step included the drying of all samples at 40 °C, followed by their disaggregation and homogenization. We collected five surface soil samples (from 5 to 25 cm depth) from forested and unforested slopes upstream of the Tinoasa Ponor, where the surface stream flows into Ciur Izbuc Cave (see Fig. 1B inset). More precisely, two samples (CI-1 and CI-4) were taken from soil covering a forested limestone area, two (CI-3, CI-5) from soil developed on sandstone, and one from the streambed (CI-2). We subjected these samples to the same set of analyses.

The magnetic susceptibility measurements were performed using a Bartington Instruments Ltd. MS 2 m and MS2B sensor. Analyses focused on high frequency to calculate frequency-dependent magnetic susceptibility (χFD), which is commonly used to identify the presence of magnetically susceptible minerals and infer processes such as diagenesis and weathering (Mullins, 1977). The total organic matter (OM) content was estimated using the loss-on-ignition method by sequential burning at 550° and expressed as a percentage (%) of the dry weight (Heiri et al., 2001). To determine the carbon (C%) and nitrogen (N%) content, we analyzed 5–10 mg of dry sediment with Vario EL cube instrument.

The particle size distribution was measured using a Horiba Laser Scattering Particle Size Analyzer (Partica LA-950). We analyzed the ashed samples using a well-established protocol to reduce uncertainties. Each sample was analyzed three times following 1-min ultrasonication (Santisteban et al., 2004).

The geochemical properties of the samples were investigated using a Niton XL 3 t 900 field portable X-Ray Fluorescence analyzer (fpXRF) mounted on a shield and used in laboratory conditions. We measured only those elements (see presentation in section 4.2) that are routinely used in sedimentary geochemistry. For all these elements, the relative percentage difference between the concentration of the certified reference material (CRM NCS DC73308) and the concentration measured was <10 %.

We analyzed by X-ray diffraction (XRD) ten samples collected from each lithological unit to investigate the mineralogical composition of the sediments and determine their provenance. The sediment samples were subjected to a slow drying process at 40 °C for 48 h, followed by grinding and homogenization to reduce the particle size to an average diameter of 5–10 μm. We utilized a Bruker D8 Advanced diffractometer, located at the Department of Geology, Babeș-Bolyai University (Cluj-Napoca, Romania). The instrument uses a CuKα type radiation ($\lambda = 1.54$ Å with Ni Kβ filter) and it was operated at 40 kV and 40 mA and the diffracted X-rays were registered by LynxEye detector. The scanning 2θ angle range was between 3.8° and 64°, with a step size of 0.02° (2θ) and a measuring time of 2 s/step. To identify the mineral phases, the X-ray patterns of the sample were compared with the International Centre for Diffraction Data Powder Diffraction Files (ICDD PDF) database using the DifracEva software (Bruker Corporation).

We determined six radiocarbon (^{14}C) ages on macro-remains of terrestrial origin (leaf, charcoal) and bulk sediments using the accelerator mass spectrometry facility at the Hertelendi Laboratory of

Environmental Studies, Debrecen, Hungary. The ages were calibrated with OxCal (v4) at 2σ range using the IntCal20 calibration curve (Reimer et al., 2020), while the age-depth model was constructed using the Bacon package (Blaauw and Christen, 2011) in R (https://cran.r-project.org/package=rbacon).

3.2. Principal component analysis

Principal component analysis (PCA) was conducted on selected geochemical, mineral magnetic, and organic matter parameters to examine the relationships between proxies and to determine which of them contribute most to sediment variability. The PCA was performed on a correlation matrix in RStudio using the 'factoextra' package (R Core Team, 2023). Significant axes were determined using the broken stick model, a method for estimating the number of significant principal components – break points.

This analysis simplifies the complexity of our data by helping to identify the most significant factors that explain the variability in sedimentary characteristics. It also reveals how specific elements or proxies group together, indicating shared sources or sedimentary processes. Furthermore, PCA identifies which combinations of proxies contribute most to sediment changes, enhancing our understanding of the underlying processes that influence the sedimentary environment in the cave.

3.3. Pollen, non-pollen palynomorphs, and charcoal analyses

We used pollen analysis to determine the past vegetation changes on samples of 0.5 cm^3 at intervals of 20 cm along the core. Sediment preparation followed the protocol of Bennett and Willis (2001). Pollen grains were identified using the atlas of Moore et al. (1991). The pollen concentration and therefore the pollen counts were extremely low, ranging between 2 and 25 grains/sample. However, non-pollen palynomorphs (NPPs), mainly fungal taxa, were common and tallied during pollen counting (van Geel et al., 2003; Shumilovskikh et al., 2021). NPPs were grouped by their nutritional strategies in i) coprophilous fungal taxa (*Sporormiella*, *Apiosordaria, Podospora*, *Chaetomium*, *Coniochaeta*, *Cercophora*) that are used to indicate past grazing activity or cultivated soils and ii) lignicolous or fungal taxa of decaying wood, including submerged wood (*Ustulina deusta, Xylomyces, Dictyosporium)*. Microscopic charcoal particles were counted on the same slides used for pollen analysis to generate information on regional-scale fire history (Whitlock and Larsen, 2001). We have transformed the pollen counts into pollen percentages by calculating the percentages based on the total sum of terrestrial pollen grains. Pollen and microcharcoal concentrations were estimated in relation to the number of *Lycopodium* tablets added and the volume of sediment and are expressed as particles/cm^3.

Macroscopic charcoal particles were counted on samples of 2 cm^3 extracted at each 10 cm interval to determine past local fire. Samples were bleached overnight and wet-sieved through a 125-μm. Charcoal morphologies were identified under a stereomicroscope and categorized into woody and herbaceous types following the methodology described in Feurdean et al. (2023). We calculated the macrocharcoal concentration (particles/cm^3) by dividing the total counts by the sediment volume, then the macrocharcoal accumulation rate (particles/cm^2/yr) by dividing the total macrocharcoal concentration by sediment deposition time (yr/cm).

4. Results

4.1. Radiocarbon dating

All ^{14}C ages occur in stratigraphic order and span the last 6500 years (Table 1). The age-depth curve shows changes in the sediment accumulation rate (SAR) at different depths. From 6500 to 3600 cal BP (128–80 cm), the accumulation rate ranged from moderate (0.02 cm/yr) to high (0.03 cm/yr). It then decreased to 0.01 cm/yr between 3500 and 1900 cal BP (80–65 cm), before reaching its peak at 0.05 cm/yr from 1900 to 1100 cal BP, corresponding to a depth of 65–25 cm (Fig. 2). In the upper part of the sedimentary sequence, the SAR dropped sharply around 1000 years ago to ~0.017 cm/yr before gradually increasing to 0.05 cm/yr.

4.2. Sediment characterization

The sedimentary sequence consists primarily of fine-grained materials, ranging from clay to very fine sand, with occasional occurrences of coarser particles (Fig. 3A). Most of the layers are composed of silt and fine sands, with variations in lamination and minor shifts in grain size. Coarse materials, including gravels, appear only at the base of the sequence in lithological unit (LU) 10. Within this part of the profile, a large limestone block fell from the cave ceiling disrupting the sedimentation. To obtain a complete sedimentary profile, we subsampled and overlapped two sections (see Fig. 3A and Fig. S1). All contacts between lithological units are either sharp or gradational, except for the unconformity surface beneath LU 10, which was deposited directly onto the cave floor. Sedimentary structures range from structureless to thinly (1–5 mm) or thickly (5–10 mm) laminated layers that are horizontal to slightly downstream inclined (less than 10°). Isolated plant remains and charcoal fragments are also visible in the profile. The deposition of these coarse- to fine-grained alluvial sediments is primarily attributed to the stream flowing and periodically flooding parts of the cave. Presently, the stream only reaches the location of this profile during flood events in autumn and spring. Nevertheless, in the past, the stream flowed at higher elevation, and the hydraulic conditions within the cave were different. As the water table in the cave area dropped over the past centuries, the stream incised the sediments, exposing prominent

Table 1
Accelerator mass spectrometry radiocarbon dating of bulk sediments for Ciur Izbuc record. The ages were calibrated using the package Bacon (Blaauw and Christen, 2011) in the "R" computing environment applying the IntCal20 (Reimer et al., 2020) calibration curve.

Sample ID	Composite depth (cm)	Material	Conventional ^{14}C age (yr BP ± 1σ)	Calibrated ages (yr BP ± 2σ)	Median age (cal yr BP ± 2σ)
C1_DeA-34,143	4.5	Charcoal	264 ± 24	428–377 (26.4 %) 322–282 (60.6 %) 169–153 (8.5 %)	297
C2_DeA-34,135	12.5	Charcoal	378 ± 24	501–426 (62.4 %) 379–320 (33.1 %)	461
C3_DeA-34,136	25.5	Charcoal	1223 ± 24	1248–1210 (14.7 %) 1179–1066 (80.7 %)	1111
C4_DeA-39,491	63	Bulk sediment	1927 ± 25	1928–1746 (95.4 %)	1872
C5_DeA-34,137	91.5	Charcoal	4185 ± 28	4838–4787 (22.8 %) 4766–4617 (72.7 %)	4695
C6_DeA-39,493	127.5	Bulk sediment	5729 ± 40	6636–6437 (91.5 %) 6426–6407 (4 %)	6517

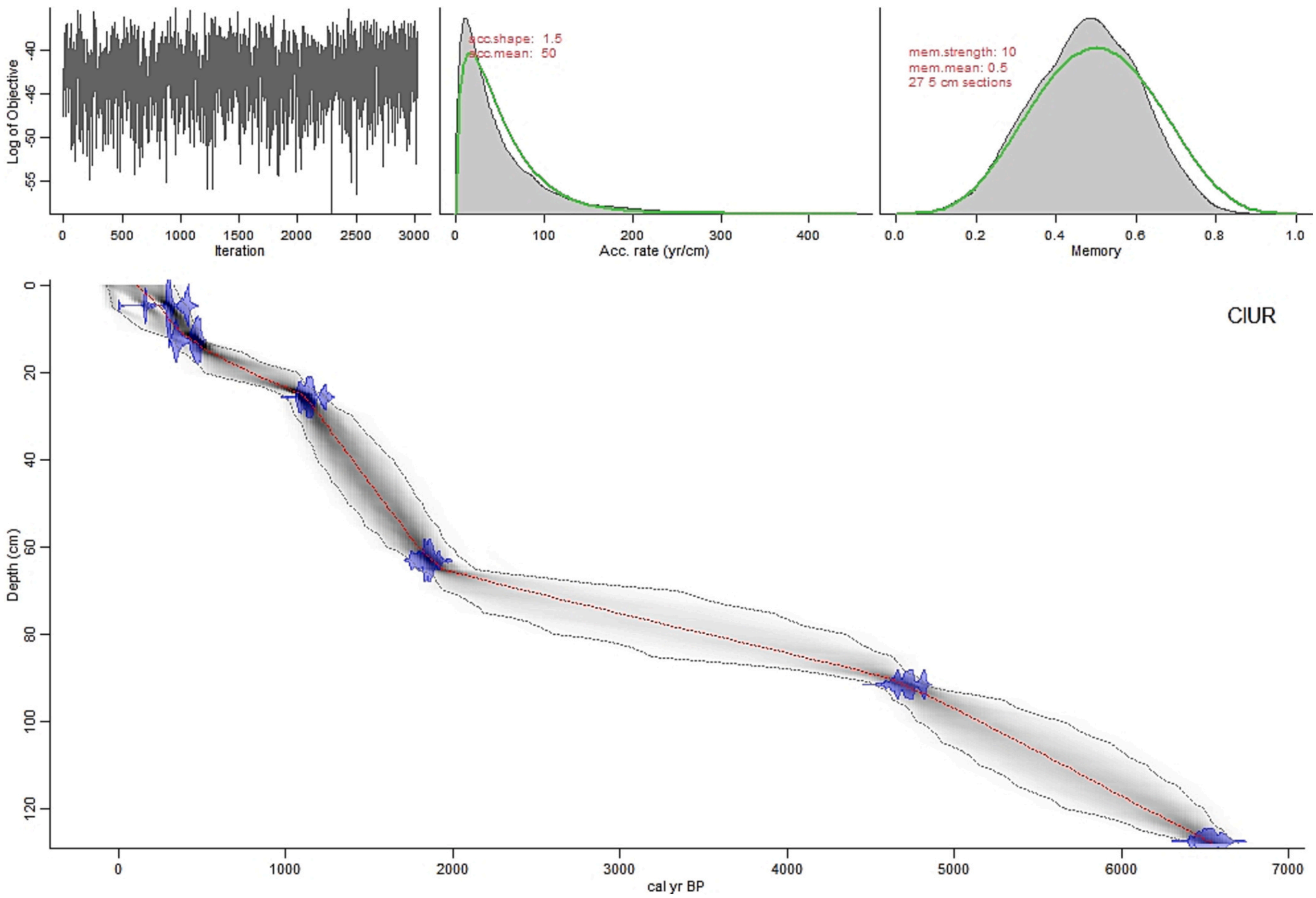

Fig. 2. Bayesian age-depth model for Ciur Izbuc, created in the "R" statistical environment (R Core Team, 2023) using the package Bacon (Blaauw and Christen, 2011). Additional information on radiocarbon samples is available in Table 1.

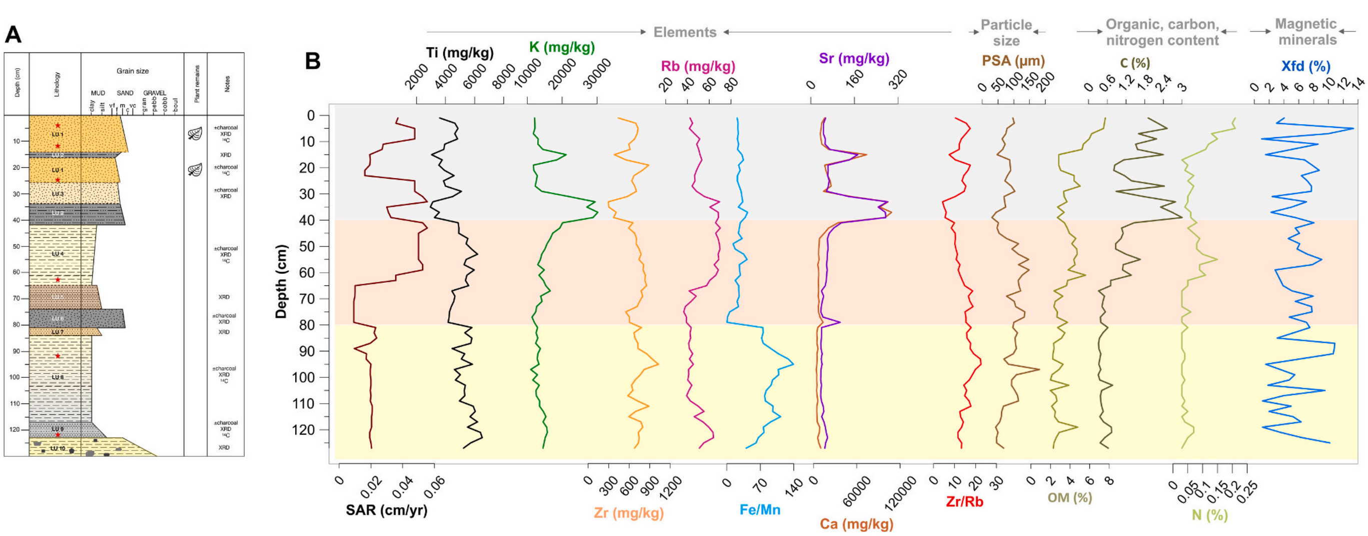

Fig. 3. A). Lithological column with the location of ^{14}C (red star) and XRD samples. B) XRF data, particle size, organic matter, carbon and nitrogen content, and magnetic minerals data plotted on depth. (For interpretation of the references to colour in this figure legend, the reader is referred to the web version of this article.)

outcrops. As expected, based on the region's geology, the XRD results indicate that quartz is the main mineralogical phase of the sedimentary profile, along with minor amounts of calcite and muscovite/illite (Fig. S2). The likely sources of quartz and muscovite/illite are the Lower Jurassic (Hettangian – Lower Sinemurian) sandstones and the soil sediments developed on these rocks, which are widely exposed in the Ciur Izbuc catchment area (Bordea et al., 1986; Ionescu and Ionescu, 1991).

In sedimentary geochemistry studies, elements such as titanium (Ti), zirconium (Zr), rubidium (Rb), calcium (Ca), strontium (Sr), potassium

(K), iron (Fe), and manganese (Mn) provide valuable insights into terrigenous input, grain size, sedimentary processes, and environmental conditions (Lowe and Walker, 2015). Titanium and Zr are immobile elements, meaning they are resistant to weathering and remain largely unaffected by post-depositional processes. They are often associated with coarse-grained sediments and are used to assess the input of terrigenous materials in various sedimentary environments. Rubidium and K indicate fine-grained material (e.g., muscovite, clay minerals) and weathering intensity, while Ca and Sr are useful for understanding carbonate contributions and type of chemical process. Zr/Rb ratio is used in sedimentary geochemistry as an indicator of grain size and sedimentary processes. Iron, Mn, and particularly Fe/Mn ratio, is critical for identifying redox conditions and biogeochemical processes within sedimentary environments. In our study, we specifically measured the Zr/Rb and Fe/Mn ratios to explore these relationships further, enhancing our understanding of sediment characteristics and depositional contexts.

The geochemical data of the sediment samples reveals a dominance of elements typical of limestone-hosted caves, with Ca exhibiting exceptionally high concentrations (17,500 mg/kg – all reported values are average), as anticipated. Elevated levels of K (15,000 mg/kg) and Fe (20,000 mg/kg) are also observed, followed by Ti (5000 mg/kg) and Mn (1560 mg/kg). Conversely, Zr (690 mg/kg), Sr (71 mg/kg), and Rb exhibit slightly lower concentrations (see Fig. 3B and Supplementary Table S1). This elemental distribution closely mirrors the composition found in soil samples collected from both forested and unforested areas within the cave's catchment zone. However, the average concentrations of Ca (7215 mg/kg) and Zr (310 mg/kg) in surface soils are approximately half those found in the cave sediments, while Fe concentrations are twice as high (39,000 mg/kg) in surface soils (see Supplemental Material, Table S1). These differences in elemental concentrations can be attributed to distinct geochemical processes. Calcium and Sr are more abundant in cave sediments due to the additional supply from limestone dissolution. Since Zr is an immobile element, its content increases as sediments accumulate in cave. The higher Fe concentration in surface soils is likely due to the iron-bearing minerals, primarily pyrite and marcasite, found in the sandstones of this age present in the Pădurea Craiului Mountains (Onac et al., 1995). Weathering of these minerals releases iron into the soil, where organic matter and microbial activity promote its accumulation. Furthermore, iron's tendency to adsorb onto soil particles, particularly clay minerals and oxides, may also contribute to its greater abundance in surface soils compared to cave sediments.

4.3. Depositional phases

Based on the age-depth model and sediment characteristics, the Ciur Izbuc sedimentary profile was divided into three depositional phases as follows:

Phase I (128–80 cm depth, 6500–3500 cal BP) is composed of a layer of gray silt followed by very fine and fine yellowish sand. Ti exhibits high values displaying a notably variable pattern marked by several peaks around 98 and 87 cm (Fig. 3). Conversely, K follows a monotonous trend with low values during this phase. Zr displays a fluctuating trend, with elevated values at depths around 110 and 95 cm. The Rb curve shows higher values in the lower part spanning from 128 to 110 cm in depth, followed by a decline up to 80 cm in depth (Fig. 3). The Zr/Rb ratio mirrors the same trend as the median particle size, with a progressing increase peaking at ~90 cm in depth, followed by a declining phase that includes a double spike before and right after ~70 cm. Conversely, the Ca and Sr curve exhibits consistently low values throughout the entire profile depicting a monotonous trend. The Fe/Mn ratio shows a variable pattern, with elevated values in the range between 80 and 128 cm, featuring two spikes at ~115 and 95 cm (Fig. 3).

The particle size analysis (PSA) describes the most dynamic variation reaching its highest values across the entire record, with a prominent peak at 98 cm. The organic matter (OM) content shows low values (<8 %), and displays a mildly oscillating pattern in the lower part of the profile, spanning from 128 to 60 cm. In this same section, C% records its lowest values in the entire record. Similarly, the N% mirrors the trends observed for C%. Although no iron minerals were detected in the XRD spectra, the χFD% indicates the presence of fine, 'viscous' magnetic minerals, predominantly pedogenic in origin. These include superparamagnetic and non-superparamagnetic grains, which exhibit an oscillating trend in this part of the sedimentary sequence, with a marked peak around 87 cm (Fig. 3). Under varying redox conditions, Fe-bearing minerals such as goethite and lepidocrocite, may form in colloidal or poorly crystalized phases at concentrations below the detection limits of X-ray instruments. This appears to be the case during Phase I, where the high Fe/Mn ratio suggests an oxygenated environment that would have promoted the precipitation of disordered, fine-grained Fe minerals in the cave sediments.

Phase II (80–40 cm, 3500–1400 cal BP) comprises a thin (7 cm) Mn-rich black, compact sandy layer followed by very fine, orange-colored sand and yellowish silt. The Ti curve exhibits slightly lower values compared with the rest of the record, with higher values in the upper part of this phase. K shows slightly elevated values illustrating an increasing trend (Fig. 3). Rb shows lower values between 80 and 65 cm and higher values from 65 to 40 cm, while Zr follows the reverse pattern. No notable peaks are visible. Ca and Sr depict a relatively stable pattern with minimal variations. The particle size shows a substantial variability between 80 and 65 cm, followed by lower values under a monotonous trend between 65 and 40 cm (Fig. 3). Notably, two peaks stand out at ~77 and ~ 67 cm. Organic matter content, as well as C% and N% registers lower values in the 80 to 65 cm, followed by an increase in the upper part, from 65 to 40 cm. The χFD% shows some decline in the prevalence of fine magnetic minerals (admixture of SP and non-SP grains), revealing a variable trend.

Phase III (40–0 cm, 1400–100 cal BP) is characterized by a gray layer of very fine sand, interbedded with alternating dark and light brown layers of very fine sand and silt. This phase exhibits distinctive characteristics in the elemental data. Ti records lower values, depicting a markedly oscillating pattern. K displays higher values, featuring notable peaks at 35 and 15 cm (Fig. 3). Zr shows exceptionally high values, outlining an increasing trend, whereas Rb values are decreasing. Ca and Sr reveal two large peaks around 35 and 20 cm. As for the particle size distribution, it follows a more dynamic pattern, featuring slightly higher values between 40 and 20 cm (Fig. 3). In this part of the profile, the OM content displays an increasing trend, with higher values in the top 20 cm. The carbon content depicts a distinct oscillation pattern (Fig. 3). Lastly, χFD% exhibits fluctuations, showing higher values in the uppermost 20 cm.

4.4. Principal component analysis

The first two components of the PCA, PC1 (44.9 %) and PC2 (16.6 %) explain 62 % of the data variance (Fig. 4). The first component (PC1+) depicts a detrital/terrigenous component with high positive values for Ti and Zr. This is inversely correlated with the PC1–, which yields negative values for Ca, Sr, K, C, and C/N ratio, indicating a carbonate-rich source. The positive axis of the PC2+ yields high values for particle size and Fe/Mn ratio indicating a component associated with redox conditions/geochemistry and changes in grain size. The negative axis of PC2– is associated with OM and N and depicts an organic matter pool (Fig. 4). The distribution of multi-proxy parameters across the depositional phases shows the association between Phase I and PC1+ direction, a strong correlation of Phase III with PC1– direction, whereas Phase II shows high variability and spreads across PC2. Fig. 4B shows the quality of representation (Cos2), a parameter which expresses how much each variable is represented in each component. Cos2 shows high values for Ca, Sr, K, and C/N variables for PC1 and N, PSA, and Rb for PC2.

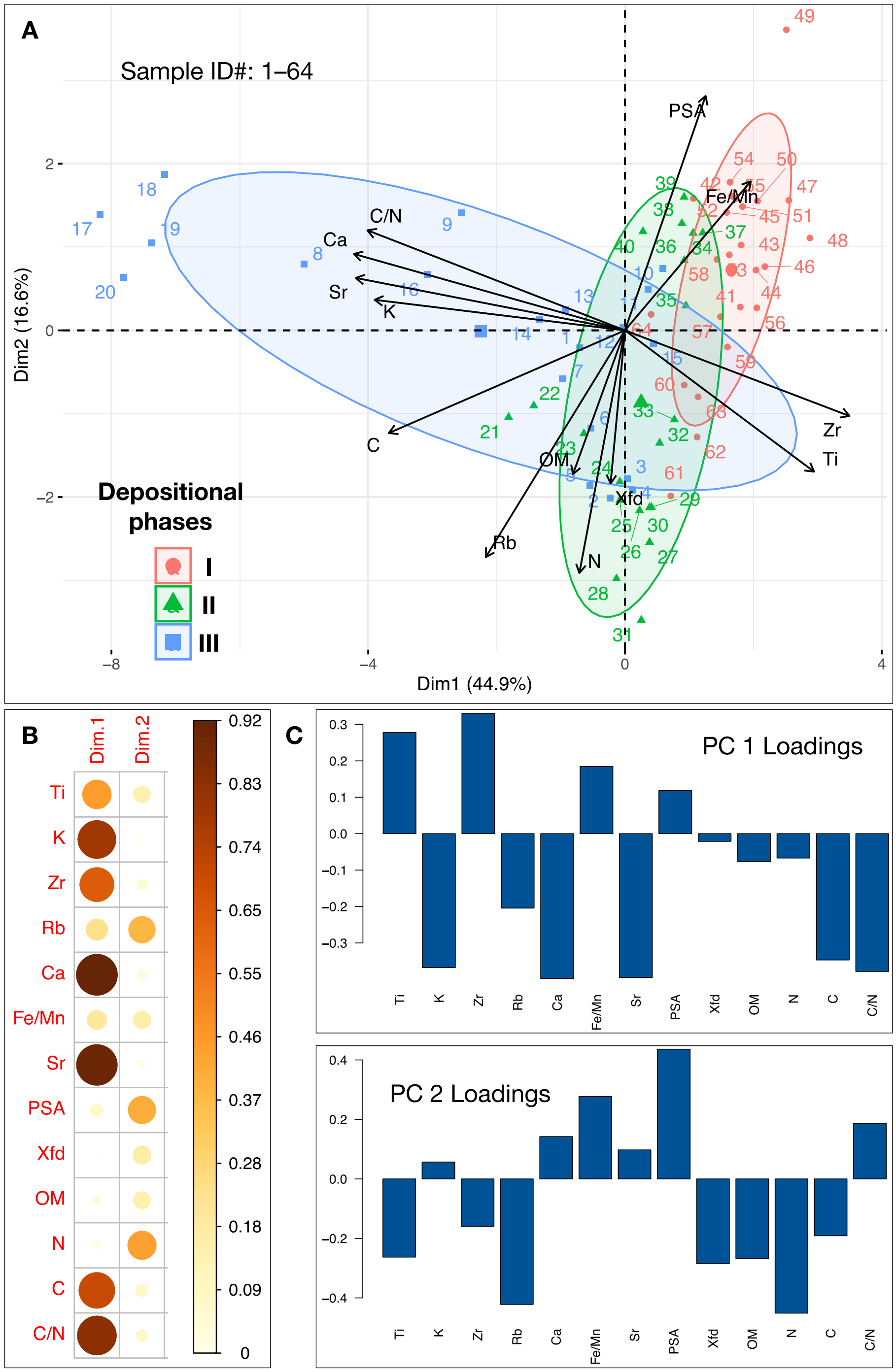

Fig. 4. A). PCA results. B) The quality of representation (cos2) of variables where larger and darker circles illustrates better quality of representation of a variable category within a specific dimension (Dim.) of the two principal components. C) Loadings for PC dimensions.

4.5. *Pollen, non-pollen palynomorphs, and charcoal*

The Ciur Izbuc sediment record exhibits extremely low pollen concentration, however NPPs and charcoal are more common throughout the record (Fig. 5). There is a close correlation between the changes in NPPs and charcoal concentrations and the sediments' lithological characteristics; therefore, we have adopted the same phases to delineate the main paleoecological changes.

4.5.1. *Phase I (128–80 cm depth, 6500–3500 cal BP)*

The samples from the lower part of the profile contain pollen typical of temperate trees such as *Corylus, Tilia*, and *Ulmus* (see Supplemental Material, Table S2). Pollen of coniferous trees (*Pinus*), as well as Poaceae, were also identified in these samples. Notably, no remains of NPPs were detected during this phase. Microcharcoal concentrations exhibited low to moderate values (4000 grains/cm^3). In contrast, the macrocharcoal concentration were the lowest within the entire record during this phase, with consistently low input of woody morphologies and a distinct peak in herbaceous morphologies between 6500 and 6200 cal BP (Fig. 5).

4.5.2. *Phase II (80–40 cm, 3500–1400 cal BP)*

This phase is characterized by the presence of tree pollen from *Carpinus* and *Ulmus*, herbaceous plants such as Asteraceae, and pollen and

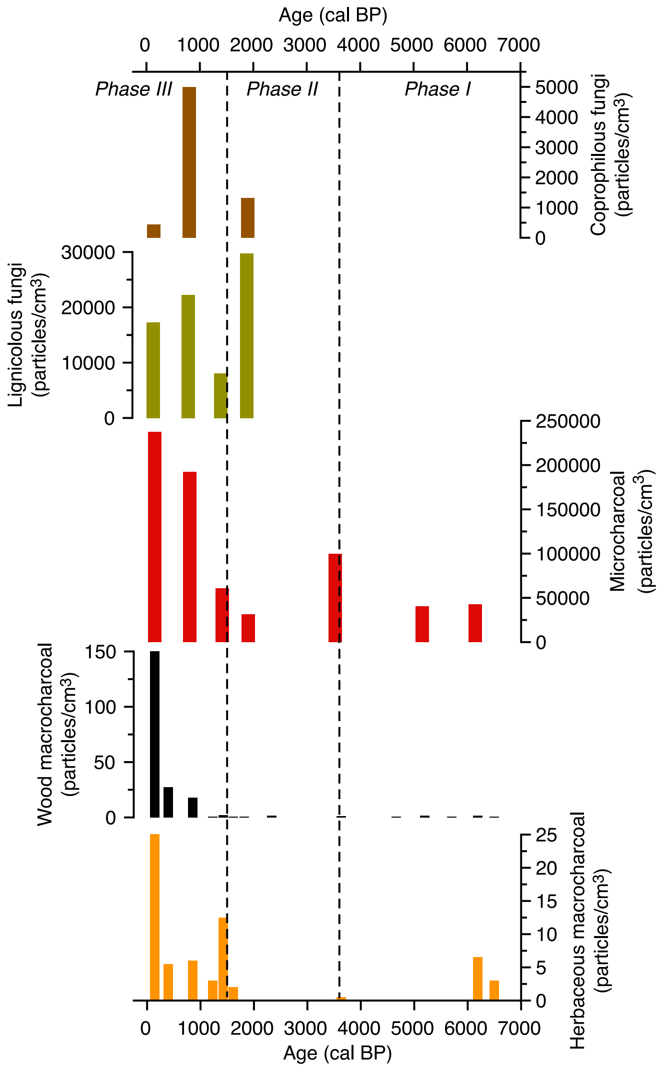

Fig. 5. Concentration of lignicolous and coprophilous fungal taxa, and the micro and macrocharcoal fragments of herbaceous and wood plants from Ciur Izbuc cave sediment.

spores from wet environments, including Cyperaceae and Polypodiaceae (see Supplemental Material, Table S2). At 1800 cal BP, there was a marked increase in the concentration of wood decaying fungal taxa, such as *Ustulina deusta* and some from *Xylomyces/Dictyosporium* (Fig. 5). Furthermore, coprophilous fungal spores, such as *Sporormiella* and *Cercophora* were also detected. During this phase, there was a slight decrease in the concentration of microcharcoal particles, whereas macrocharcoal concentration remained generally low, except for small rise observed at ~1425 cal BP primarily composed of herbaceous charcoal morphologies.

4.5.3. *Phase III (40–0 cm, 1400–100 cal BP)*

In this phase, the pollen analysis reveals the presence of *Fagus, Carpinus, Ulmus*, and *Picea,* alongside Cyperaceae and Polypodiaceae and sporadic occurrence of cereal pollen (see Supplemental Material, Table S2). Notably, the concentration of wood decay fungal taxa remained consistently high (Fig. 5). Concurrently, the concentration and diversity of coprophilous fungal taxa such as *Apiosordaria, Podospora, Chaetomium,* and *Coniochaeta* reached their maximum values between 1417 and 400 cal BP. Microcharcoal concentrations increased markedly during this phase, with the highest values observed between 850 and 150 cal BP. This paralleled the highest values in macrocharcoal concentration primarily consisting of woody morphologies including numerous large pieces (Fig. 5).

5. Discussion

The depositional architecture of cave sediments is influenced by the dynamics of fluvial processes, transport pathways and cave morphology (Bosch and White, 2004). The Ciur Izbuc Cave sediment profile enables the identification of periods when deposition changed, providing an opportunity to explore connections with regional and continental scale mid and late Holocene paleoclimatic and paleoenvironmental changes.

5.1. *Sedimentary depositional phases*

The investigated profile reveals three distinct depositional phases spanning the last 6500 cal BP.

5.1.1. *Phase I (6500–3500 cal BP): intermittently unstable, energetic depositional environment*

The first depositional phase is marked by elevated concentrations of immobile minerogenic elements (Ti, Zr), which prevail over organic matter and other elements. This suggests intense surface weathering and efficient sediment transport into the cave. Calcium and Sr exhibit similar trends, indicating weak limestone dissolution processes during this period. Although sediment accumulation rate is moderate when compared with the following intervals, it remains steady (Fig. 6). High values in sediment grain size suggest deposition of coarser material, and therefore an energetic depositional environment. The magnetic susceptibility (χFD%) also indicates some presence of fine magnetic minerals, likely from top-soil erosional source (Dearing, 1999). The high Fe/Mn ratio suggests a highly oxygenated environment, which could explain the very low abundance of organic matter throughout this phase (Fig. 6).

Collectively, these proxies depict a dynamically connected surface and subsurface system. During this phase, a well-developed hydrographic network likely facilitated the transport and deposition of coarse sediment particles. This is supported by Ti, Zr/Rb ratio, and particle size curves, which reflect short-term, highly minerogenic depositional events in an intermittently unstable environment (Fig. 6).

5.1.2. *Phase II (3500–1400 cal BP): calm depositional conditions followed by energetic activity*

In the early part of this second phase, sediment geochemistry and granulometry indicate a decrease in water flow energy, leading to reduced deposition of mainly fine-grained sediment, such as clay and silt. These finer particles have smaller pore spaces, restricting oxygen diffusion into the sediment, as reflected by the very low Fe/Mn ratio. In contrast, between 1900 and 1500 cal BP, the lower Zr/Rb ratio suggests a more active hydrodynamic system with predominantly coarse-grained sediment transport (see Figs. 3 and 6). The peak in Ti concentration during this period may indicate a shift in sediment supply or hydrodynamic conditions that favor the transport of Ti-rich coarse sediments, as supported by a broad peak in the particle size distribution curve. This aligns with the mineral magnetic assemblages (χFD%), denoting a stable input of magnetically enriched material coming from surface soil erosion. The sediment accumulation rate curve shows low, stable values from 3500 to 2000 cal BP, followed by a sudden shift to exceptionally high values between 1900 and 1500 cal BP (Fig. 6).

Organic matter content remains low throughout most of the interval, likely due to drier conditions and reduced surface runoff, which limited the entry of organic material into the cave. The only notable peak occurs between 1900 and 1600 cal BP, signaling a wetter period with increased transport, as also indicated by the SAR and Ti curves (Fig. 6). The increasing levels of K towards the end of this interval suggest that fine-grained sediments were settling as the system transitioned to low-energy water flow that characterized the onset of Phase III.

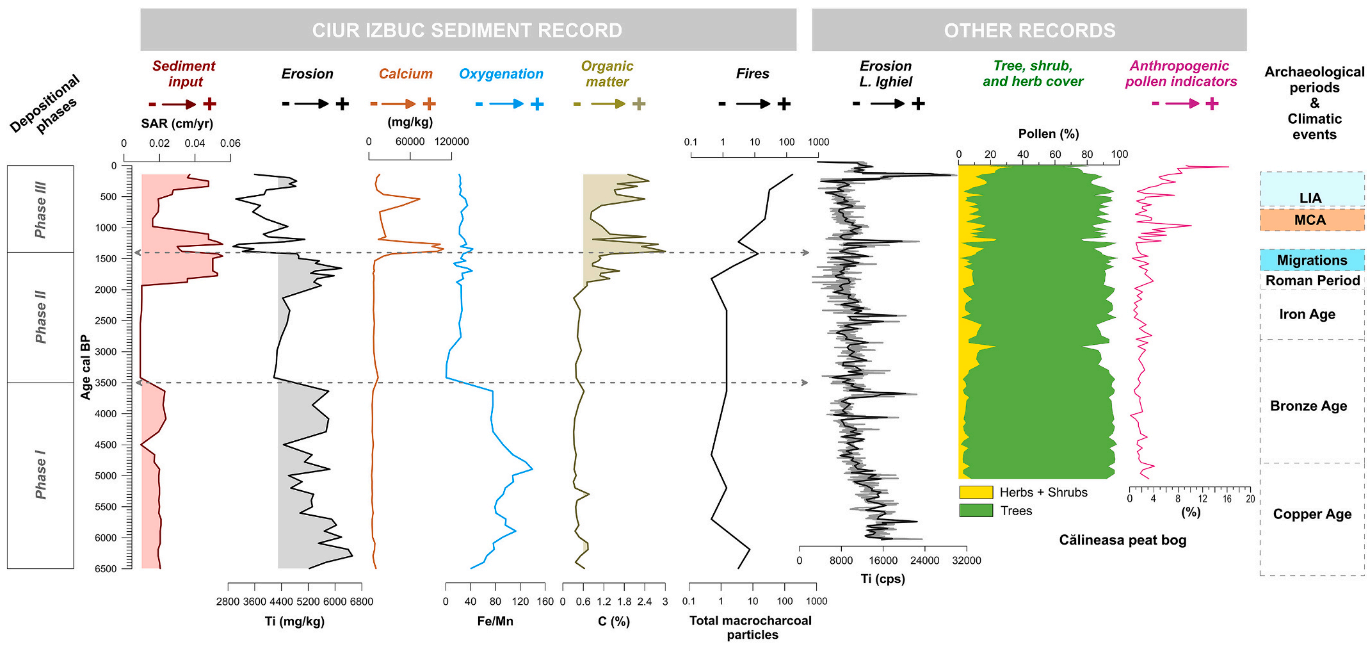

Fig. 6. Comparison of selected geochemical and biological proxies from Ciur Izbuc Cave with other records from the region, including Ti from Lake Ighiel (Haliuc et al., 2017) and vegetation changes and human impacts based on pollen from Călineasa Peat Bog (Feurdean et al., 2009). The X-axis of the total macrocharcoal plot is on a logarithmic scale. MCA = Medieval Climatic Anomaly, LIA = Little Ice Age.

5.1.3. *Phase III (1400–100 cal BP): dynamic depositional environment*

The third phase features a distinct depositional architecture, deviating in character from earlier patterns. Minerogenic particles display a decreasing trend with occasional spikes, indicating intermittent transport-deposition activity. Concurrently, higher values in mineral magnetic assemblages at 1200 and 250 cal BP, suggest input of coarse-grained surface sediments, as reflected by peaks in the Ti and PSA curves (see Figs. 3 and 6). These observations align with the sediment accumulation curve and organic matter content trends, all revealing higher values up to 1200 cal BP, a significant drop around 1000 cal BP, and a subsequent increase after 500 cal BP. Ti and Ca exhibit opposite trends around ~1300 and ~ 550 cal BP, supporting the idea that percolation water, rather than catchment runoff, was recharging the cave stream. The peaks in organic matter at these times suggest that the water was acidified by biogenic CO_2 from the soil, leading to more aggressive dissolution of limestone bedrock (reflected by high Ca and Sr) and reduced erosional input (indicated by low Ti). The Fe/Mn ratio remains stable and very low, due to overall larger amount of organic matter compared to the previous depositional phases.

Notably, during these two events, elevated K levels suggest an influx of fine-grained muscovite/illite (identified through X-ray diffraction; see Fig. 2S), which can be transported in suspension under low-energy flow conditions. This is further supported by low Zr values and a low Zr/Rb ratio (Fig. 3). Sediment accumulation rates are also reduced during these periods.

These indicators, collectively depict a dynamic depositional environment, marked by two periods of increased weathering and sediment transport, as well as two intervals of more intensified bedrock dissolution, all responding to fluctuations in surface environmental conditions.

5.2. *Cave sediment deposition, surface erosion, climate, environmental changes, and human activities*

In the mid-Holocene, a documented climate change towards cooler and more humid conditions occurred at a continental scale (Wanner et al., 2008; Debret et al., 2009; Fletcher et al., 2013; Perşoiu et al., 2017). This shift is evident in multiple paleoclimatic records from the Carpathians (Feurdean et al., 2008; Magyari et al., 2009; Onac et al., 2015; Toth et al., 2015; Diaconu et al., 2017; Perşoiu et al., 2017; Panait et al., 2017; Ramos-Román et al., 2022) and was linked to changes in atmospheric circulation, particularly a shift towards a more positive North Atlantic Oscillation state (Perşoiu et al., 2017; Drăguşin et al., 2023) that led to increased autumn and early winter precipitation in western Romania due to the prevalence of Mediterranean cyclones.

Between 6500 and 3500 cal BP, the Ciur Izbuc record indicates a dynamic depositional environment, marked by intensified surface erosion in the cave's catchment area, leading to the deposition of sediments with a wide range of grain sizes rich in detrital elements and topsoil material (Fig. 6). The pronounced erosion, as indicated by high Ti values, during the first 800 years (6500–5700 cal BP) suggests overall wetter conditions and higher-energy depositional processes. Shifts from organic to minerogenic sedimentation around 6000 cal BP in nearby lakes like Ştiucii and Ighiel were similarly interpreted by Feurdean et al. (2013a), Haliuc et al. (2017), and Hutchinson et al. (2024) as driven by increased wetness and intensified erosion.

Decadal-scale intervals of drier conditions, reduced runoff, and less erosion between 5700 and 4500 cal BP caused Ti values to decrease (Fig. 6), indicating weaker sediment input during this time. This aligns with hydroclimate reconstructions from lake and peat bog sites located east and north of Ciur Izbuc Cave, all of which point to dry conditions during this period (Feurdean et al., 2008; Gałka et al., 2016; Diaconu et al., 2017).

The paucity of pollen in the record at Ciur Izbuc does not allow accurate land cover reconstruction. However, other pollen records in the Apuseni Mountains (Fig. 6) indicate relatively stable forest cover with a dynamic species composition dominated by *Corylus-Picea* before 4800 cal BP and *Carpinus-Fagus-Picea* after this time (Bodnariuc et al., 2002; Fărcaş et al., 2003; Feurdean and Willis, 2008; Feurdean et al., 2009). The charcoal record at Ciur Izbuc indicates low burning activity in the landscape around the cave (Fig. 5). Thus, human impact through deforestation and the use of fire appears to have had a limited impact on the moderate sediment delivery into the cave. This conclusion is supported by archaeological evidence that has only recorded human settlements ~30 km north of our cave site (Savu and Gogâltan, 2021).

From 3500 to 2000 cal BP, the very low cave sediment accumulation rate reflects calm surface dynamics and a stable depositional environment. In contrast, between 2000 and 1100 cal BP the cave sediment sequence shows evidence of runoff-derived erosive minerals, along with elevated concentrations of ascospores of the wood decay fungal taxa, mainly *Ustulina deusta* (Hartmann et al., 2007). This indicates increased rainfall and the transport of material from the forest floor into the cave through runoff (van Geel et al., 2003). Furthermore, we observed enhanced fire activity, as indicated by elevated concentrations of micro and macrocharcoal concentrations, alongside a slight rise in grazing activity (coprophilous fungal spores) at Ciur Izbuc (Fig. 5). A period of reduced rainfall and weaker surface runoff around ~1300 cal BP is indicated by low Ti and SAR values. The deposition of finer sediments rich in organic matter during this time is interpreted as being sourced from percolation water (high Ca and Sr values from limestone dissolution) rather than from cave stream and may have been driven by increased human activity in the catchment area (Fig. 6). There is documented evidence of extensive deforestation and extension of agropastoral activities in the Apuseni Mountains around 2000 cal BP (Bodnariuc et al., 2002; Fărcaş et al., 2003; Feurdean and Willis, 2008; Feurdean et al., 2009). Therefore, the observed changes in Ciur Izbuc Cave's sediments likely reflect increased human activity in the area surrounding the cave during the following historical periods: Roman (2000–1700 cal BP), and Migration periods (1700–1400 cal BP). Noteworthy archaeological finds, particularly from the Late Bronze and Iron Age at caves such as Meziad, Unguru Mare, Mișid, Igrița, include bronze artifacts, amber, ceramic vessels, among others, discovered in diverse ritual or mundane contexts (Ghemiș, 2021) (Fig. 6).

The reduction in cave sediment input and a clear drop in Ti concentration recorded between 1200 and 500 cal BP, partly coincides with the Medieval Climatic Anomaly, a period characterized by overall warmer and wetter climatic conditions (Büntgen et al., 2011; Feurdean et al., 2015). Although these conditions would typically lead to higher SAR and increased Ti levels, the partial infill of the Tinoasa Ponor-a key sinking point for drainage-likely restricted the amount of sediment entering the cave, leading to lower SAR and reduced Ti input.

During this interval, there was a noticeable increase in the concentration and diversity of coprophilous and wood decay fungal taxa, as well as micro and macrocharcoal particles in Ciur Izbuc's sediments (Fig. 5). A marked intensification in pastoral activity attributed to warmer summers and a longer grazing seasons, was documented in the Apuseni region (Fig. 6 and Feurdean et al., 2009). Within the cave, a small ceramic fragment dated ~500 cal BP was uncovered. These findings suggest a higher level of human activity in the surrounding landscape.

Between 500 and 100 cal BP, the sediment deposition rate and Ti concentration experience an increase advocating for intensified surface erosion, which mirrors a similar pattern noticed in the Lake Ighiel record (Fig. 6). There is also an uptick in the organic matter content and the concentration of micro and macrocharcoal, particularly woody particles, whereas the concentration of coprophilous and wood decay fungal taxa remains considerable (Fig. 5). These results imply the intensification of burning in the surrounding landscape and increased surface sediment runoff into the cave. This interval, partly coincides with the Little Ice Age, characterized by cold and dry conditions and an increase in climate extremes in Romania (Popa and Kern, 2009; Onac et al., 2015; Florescu et al., 2017; Haliuc et al., 2017; Perșoiu and Perșoiu, 2018; Longman et al., 2019). Paleoecological reconstructions from the Romanian Carpathians document a greater landscape fragmentation as we approach the present day (Bodnariuc et al., 2002; Fărcaş et al., 2003; Tanţău et al., 2011; Feurdean et al., 2013b). Therefore, changes observed over the past two millennia in Ciur Izbuc catchment area, and subsequent responses in the underground system, may be attributed to the intensification of human activities somehow facilitated by climatic conditions (Fig. 6).

6. Conclusions

The lithological, geochemical, mineral magnetic, organic matter, non-pollen palynomorphs, and charcoal analysis of Ciur Izbuc Cave's sediment provide an important record of paleoenvironmental and hydrodynamic changes over the past 6500 years. Based on this multi-proxy analysis, the following conclusions can be drawn:

1) The earliest phase of our record (6500–3500 cal BP) marks the transition from the mid- to late Holocene. It depicts a dynamic system with a constant connection between surface and subsurface leading to moderate-to-high erosion and subsequent low-to-moderate sediment accumulation rates.
2) The second depositional phase consists of two distinct intervals with a contrasting evolution. From 3500 to 2000 cal BP low sediment accumulation under reduced water flow indicates a calm cave environment, reflecting the stable climate conditions. In contrast, the sequence accumulated between 2000 and 1400 cal BP is characterized by runoff-derived eroded minerogenic sediments, anthropogenic deforestation, burning, and grazing in the region, abundantly documented in the Carpathians since the late Bronze Age. These anthropogenic impacts likely modified the Ciur Izbuc catchment and influenced the signal preserved in the cave sediments.
3) The third phase (1400–100 cal BP) exhibits a different depositional architecture, marked by complex hydrological dynamics. During this time sporadic, yet intense, physical erosion events occur in response to short-term shifts in climatic conditions (~1200 and ~ 300 cal BP). Increased concentrations of charcoal particles and lignicolous and coprophilous fungal taxa suggest anthropogenically enhanced erosion from 1400 cal BP, which intensified notable after 300 cal BP.

The episodic depositional events identified in the Ciur Izbuc Cave record appear to be closely linked to climate events that occurred at regional scale over the past 6500 years. Our study emphasizes the importance of a multi-proxy approach in cave sediment records in understanding the dynamics of sediment deposition in caves, documenting transformations in the local environment, and highlighting their relationship with past climatic changes. Future research will extend this approach by integrating archaeological and paleontological evidence to construct a detailed picture of past human activities and the evolving environmental backdrop.

CRediT authorship contribution statement

Bogdan P. Onac: Writing – review & editing, Writing – original draft, Visualization, Methodology, Investigation, Conceptualization. **Angelica Feurdean:** Writing – review & editing, Investigation, Formal analysis, Data curation. **Aritina Haliuc:** Writing – original draft, Visualization, Formal analysis, Data curation, Conceptualization. **Simon M. Hutchinson:** Writing – review & editing, Formal analysis, Data curation. **Ferenc L. Forray:** Investigation, Visualization, Writing – review & editing. **Andrea Demjén:** Investigation, Data curation. **Adriana Vulpoi:** Investigation, Data curation. **Răzvan Dumbravă:** Visualization, Resources. **Adrienn Lőrincz:** Investigation, Data curation. **Călin Ghemiș:** Investigation, Data curation. **Augustin Nae:** Investigation, Data curation. **Viorel T. Lascu:** Resources, Methodology, Conceptualization. **Florin Gogâltan:** Investigation, Data curation. **Ioana N. Meleg:** Writing – review & editing, Project administration, Methodology, Funding acquisition, Conceptualization.

Declaration of competing interest

The authors declare that they have no competing financial interests or personal relationships that could have appeared to influence the work reported in this paper.

Acknowledgments

This work was funded by a grant from the Romanian Ministry of Education and Research, CNCS/CCCDI–UEFISCDI, project number PN-III-P4-ID-PCE-2020-0518-P, within PNCDI III to INM. We express our gratitude to the Speodava Caving Club in Ștei (Romania) for assisting during our fieldwork. We thank Rafał Kiełczewski for valuable help in the laboratory and Horea Meleg for creating the map of Romania.

Appendix A. Supplementary data

Supplementary data to this article can be found online at https://doi.org/10.1016/j.palaeo.2024.112672.

Data availability

All data used in this research are available in the Supplementary file.

References

Arriolabengoa, M., Iriarte, E., Aranburu, A., Arrizabalaga, A., 2015. Provenance study of endokarst fine sediments through mineralogical and geochemical data (Lezetxiki II cave, northern Iberia). Quat. Int. 364, 231–243. https://doi.org/10.1016/j.quaint.2014.09.072.

Bădăluţă, C.-A., Perşoiu, A., Ionita, M., Piotrowska, N., 2020. Stable isotopes in cave ice suggest summer temperatures in east-Central Europe are linked to Atlantic Multidecadal Oscillation variability. Clim. Past 16, 2445–2458. https://doi.org/10.5194/cp-16-2445-2020.

Bădescu, D., 1986. Le karst des Monts Padurea Craiului et le reseau Tinoasa-Ciur-Topliţa de Roşia (Roumanie). Karstologia 7, 41–48.

Bennett, K., Willis, K.J., 2001. Pollen. In: Birks, H.J.B., Last, W.M. (Eds.), Tracking Environmental Change Using Lake Sediments, vol. 3. Springer, Dordrecht, pp. 5–32. Terrestrial, Algal, and Siliceous Indicators.

Blaauw, M., Christen, J.A., 2011. Flexible paleoclimate age-depth models using an autoregressive gamma process. Bayesian Anal. 6 (3), 457–474. https://cran.r-project.org/package=rbacon.

Bodnariuc, A., Bouchette, A., Dedoubat, J.J., et al., 2002. Holocene vegetational history of the Apuseni Mountains, Central Romania. Quat. Sci. Rev. 21, 1465–1488. https://doi.org/10.1016/S0277-3791(01)00117-2.

Borda, D.R., Cociuba, I., Epure, L., Cruceru, N., Meleg, I.N., 2022. The interplay of environment and biota in assessing the freshwater quality in karst. Diversity 14, 475. https://doi.org/10.3390/d14060475.

Bordea, S., Bordea, J., Mantea, G., Costea, C., 1986. Geological map of Romania, 1: 50.000, L-34-45-B, Zece Hotare (40b). Institutul de Geologie și Geofizică, Bucharest.

Bosch, R.F., White, W.B., 2004. Lithofacies and transport of clastic sediments in karstic aquifers. In: Sasowsky, I.D., Mylroie, J. (Eds.), Studies of Cave Sediments. Kluwer, New York, pp. 1–22.

Büntgen, U., Tegel, W., Nicolussi, K., McCormick, M., Frank, D., Trouet, V., Kaplan, J.O., Herzig, F., Heussner, K.-U., Wanner, H., Luterbacher, J., Esper, J., 2011. 2500 years of European climate variability and human susceptibility. Science 331, 578–582. https://doi.org/10.1126/science.1197175.

Busuioc, A., Dobrinescu, A., Birsan, M.V., Dumitrescu, A., Orzan, A., 2015. Spatial and temporal variability of climate extremes in Romania and associated large-scale mechanisms. Int. J. Climatol. 35, 1278–1300. https://doi.org/10.1002/joc.4054.

Chiriloaei, F., Rădoane, M., Perşoiu, I., Popa, I., 2012. Late Holocene history of the Moldova River Valley, Romania. Catena 93, 64–77. https://doi.org/10.1016/j.catena.2012.01.008.

Chu, W., 2018. The Danube corridor hypothesis and the Carpathian Basin: Geological, environmental and archaeological approaches to characterizing Aurignacian dynamics. J. World Prehist. 31, 117–178. https://doi.org/10.1007/s10963-018-9115-1.

Cleary, D.M., Onac, B.P., Tanţău, I., Forray, F.L., Wynn, J.G., Ionita, M., Tămaş, T., 2018. A guano-derived δ^{13}C and δ^{15}N record of climate since the medieval warm period in north-West Romania. J. Quat. Sci. 33, 677–688. https://doi.org/10.1002/jqs.3044.

Clottes, J., Besesek, M., Gély, B., Ghemiş, C., Kenesz, M., Lascu, V.T., Meyssonnier, M., Philippe, M., Plichon, V., Prud'homme, F., Radu, V.A., Rus, T., Tociu, R.L., 2013. Découvert d'une nouvelle grotte ornée paléolithique en Roumanie (département du Bihor). Palethnologie 5. https://journals.openedition.org/palethnologie/2754.

Dearing, J., 1999. Environmental Magnetic Susceptibility. Using the Bartington MS2 System, 2nd ed. Chi Publishing, Kenilowort h.

Debret, M., Sebag, D., Crosta, X., Massei, N., Petit, J.-R., Chapron, E., Bout-Roumazeilles, V., 2009. Evidence from wavelet analysis for a mid-Holocene transition in global climate forcing. Quat. Sci. Rev. 28 (25–26), 2675–2688. https://doi.org/10.1016/j.quascirev.2009.06.005.

Diaconu, A.C., Toth, M., Lamentowicz, M., Heiri, O., Kuske, E., Tanţău, I., Panait, A.-M., Braun, M., Feurdean, A., 2017. How warm? How wet? Hydroclimate reconstruction of the past 7500 years in northern Carpathians, Romania. Palaeogeogr. Palaeoclimatol. Palaeoecol. 482, 1–12. https://doi.org/10.1016/j.palaeo.2017.05.007.

Drăguşin, V., Staubwasser, M., Hoffmann, D.L., Ersek, V., Onac, B.P., Veres, D., 2014. Constraining Holocene hydrological changes in the Carpathian–Balkan region using speleothem δ^{18}O and pollen-based temperature reconstructions. Clim. Past 10 (4), 1363–1380. https://doi.org/10.5194/cp-10-1363-2014.

Drăguşin, V., Ersek, V., Fleitmann, D., Ionita, M., Onac, B.P., 2023. Winter hydroclimate contrasts between southern and northern Europe at ~5.2 ka. Palaeogeogr. Palaeoclimatol. Palaeoecol. 632, 111863. https://doi.org/10.1016/j.palaeo.2023.111863.

Fărcaş, S., Tanţău, I., Bodnariuc, A., 2003. The Holocene human presence in Romanian Carpathians, revealed by the palynological analysis. Wüzburger Geograph. Manuskripte 63, 113–130.

Farrant, A.R., Smart, P.L., 2011. Role of sediment in speleogenesis; sedimentation and paragenesis. Geomorphology 134, 79–93. https://doi.org/10.1016/j.geomorph.2011.06.006.

Feurdean, A., Willis, K.J., 2008. The usefulness of a long-term perspective in assessing current forest conservation management in the Apuseni Natural Park, Romania. For. Ecol. Manag. 256, 421–430. https://doi.org/10.1016/j.foreco.2008.04.050.

Feurdean, A., Klotz, S., Mosbrugger, V., Wohlfarth, B., 2008. Pollen-based quantitative reconstructions of Holocene climate variability in NW Romania. Palaeogeogr. Palaeoclimatol. Palaeoecol. 260, 494–504. https://doi.org/10.1016/j.palaeo.2007.12.014.

Feurdean, A.N., Willis, K.J., Astaloş, C., 2009. Legacy of the past land-use changes and management on the 'natural' upland forest composition in the Apuseni Natural Park, Romania. The Holocene 19, 967–981. https://doi.org/10.1177/0959683609337358.

Feurdean, A., Perşoiu, A., Pazdur, A., Onac, B.P., 2011. Evaluating the palaeoecological potential of pollen recovered from ice in caves: a case study from Scărişoara Ice Cave, Romania. Rev. Palaeobot. Palynol. 165, 1–10. https://doi.org/10.1016/j.revpalbo.2011.01.007.

Feurdean, A., Liakka, J., Vannière, B., Marinova, E., Hutchinson, S.M., Mosburgger, V., Hickler, T., 2013a. 12,000-years of fire regime drivers in the lowlands of Transylvania (Central-Eastern Europe): a data-model approach. Quat. Sci. Rev. 81, 48–61. https://doi.org/10.1016/j.quascirev.2013.09.014.

Feurdean, A., Parr, C.L., Tanţău, I., Fărcaş, S., Marinova, E., Perşoiu, I., 2013b. Biodiversity variability across elevations in the Carpathians: parallel change with landscape openness and land use. The Holocene 23 (6), 869–881. https://doi.org/10.1177/0959683612474482.

Feurdean, A., Galka, M., Kuske, E., Tantău, I., Lamentowicz, M., Florescu, G., Liakka, J., Hutchinson, S.M., Mulch, A., Hickler, T., 2015. Last Millennium hydro-climate variability in Central–Eastern Europe (Northern Carpathians, Romania). The Holocene 25, 1179–1192. https://doi.org/10.1177/0959683615580197.

Feurdean, A., Vachula, R.S., Hanganu, D., Stobbe, A., Gumnior, M., 2023. Charcoal morphologies and morphometrics of a Eurasian grass-dominated system for robust interpretation of past fuel and fire type. Biogeosciences 20, 5069–5085. https://doi.org/10.5194/bg-20-5069-2023.

Fletcher, W.J., Debret, M., Goni, M.F.S., 2013. Mid-Holocene emergence of a low-frequency millennial oscillation in western Mediterranean climate: implications for past dynamics of the North Atlantic atmospheric westerlies. The Holocene 23 (2), 153–166. https://doi.org/10.1177/0959683612460783.

Florescu, G., Hutchinson, S.M., Kern, Z., Cristea, I.A., Feurdean, A., 2017. Last 1000 years of environmental history in southern Bucovina, Romania: a high-resolution multi-proxy lacustrine archive. Palaeogeogr. Palaeoclimatol. Palaeoecol. 473, 26–40. https://doi.org/10.1016/j.palaeo.2017.01.047.

Forray, F.L., Onac, B.P., Tanţău, I., Wynn, J.G., Tămaş, T., Coroiu, I., Giurgiu, A.M., 2015. A late Holocene environmental history of a bat guano deposit from Romania: an isotopic, pollen, and microcharcoal study. Quat. Sci. Rev. 127, 141–154. https://doi.org/10.1016/j.quascirev.2015.05.022.

Gałka, M., Tanţău, I., Ersek, V., Feurdean, A., 2016. A 9000year record of cyclic vegetation changes identified in a montane peatland deposit located in the Eastern Carpathians (Central-Eastern Europe): Autogenic succession or regional climatic influences? Palaeogeogr. Palaeoclimatol. Palaeoecol. 449, 52–61.

Ghemiş, C., 2021. Istoricul și stadiul actual al cercetărilor arheologice din endocarstul Munților Pădurea Craiului. Stud. Histor. Transylvaniensia 3, 283–312.

Gillieson, D., 2021. Caves: Processes, development, and management, 2nd ed. Wiley Blackwell, Chichester.

Gogâltan, F., Ghemiș, C., Demjén, A., Gál, S., Meleg, I.N., Onac, B.P., Haliuc, A., Nae, A., Lascu, V.T., Dumbravă, R., Rus, T., Lőrincz, A., Botha, Z., Oana, M., Mereuță, D., 2023. Luncasprie, com. Dobrești, jud. Bihor, Punct: Peștera Izbucul Topliței de Vida. In: Cronica cercetărilor arheologice. Campania 2022. A LVII-a Sesiune Naţională de Rapoarte Arheologice, 29-31 mai 2022, Târgoviște, pp. 237–241.

Groza, G., 2008. Flora și vegetația Munților Pădurea, Craiului. ed. Risoprint, Cluj-Napoca.

Haliuc, A., Veres, D., Brauer, A., Hubay, K., Hutchinson, S.M., Begy, R., Braun, M., 2017. Palaeohydrological changes during the mid and late Holocene in the Carpathian area, Central-Eastern Europe. Glob. Planet. Chang. 152, 99–114. https://doi.org/10.1016/j.gloplacha.2017.02.010.

Hartmann, G., Nienhaus, F., Butin, H., 2007. Farbatlas Waldschäden. Diagnose von Baumkrankheiten, Stuttgart, Ulmer (in German).

Heiri, O., Lotter, A.F., Lemcke, G., 2001. Loss on ignition as a method for estimating organic and carbonate content in sediments: Reproducibility and comparability of results. J. Paleolimnol. 25 (1), 101–110. https://doi.org/10.1023/A:1008119611481.

Hunt, C.O., Gilbertson, D.D., Hill, E.A., Simpson, D., 2015. Sedimentation, re-sedimentation and chronologies in archaeologically-important caves: problems and prospects. J. Archaeol. Sci. 56, 109–116. https://doi.org/10.1016/j.jas.2015.02.030.

Hutchinson, S.M., Haliuc, A., Feurdean, A., 2024. Tracing climate and human-driven erosional activity in the Transylvania lowlands (Central-Eastern Europe) during the Holocene. The Holocene 34 (9), 1266–1277. https://doi.org/10.1177/09596836241254477.

Ianovici, V., Borcoş, M., Bleahu, M., Patrulius, D., Lupu, M., Dimitrescu, R., 1976. Geologia Munţilor Apuseni. Editura Academiei R.S.R, Bucureşti.

Ionescu, G., Ionescu, C., 1991. Considerations concerning the gypsum occurrence in the Ciur-Izbuc Cave (Pădurea Craiului Mountains, Romania). Theoret. Appl. Karstol. 4, 183–187.

Longman, J., Veres, D., Ersek, V., Haliuc, A., Wennrich, V., 2019. Runoff events and related rainfall variability in the Southern Carpathians during the last 2000 years. Sci. Rep. 9, 5334. https://doi.org/10.1038/s41598-019-41855-1.

Lowe, J.J., Walker, M.J.C., 2015. Reconstructing Quaternary Environments. Routledge, New York.

Magyari, E., Buczko, K., Jakab, G., Braun, M., Pal, Z., Karatson, D., Pap, I., 2009. Palaeolimnology of the last crater lake in the Eastern Carpathian Mountains: a multiproxy study of Holocene hydrological changes. Hydrobiologia 631 (1), 29–63. https://doi.org/10.1007/s10750-009-9801-1.

McAdams, C., Morley, M.W., Fu, X., Kandyba, A.V., Derevianko, A.P., Nguyen, D.T., Doi, N.G., Roberts, R.G., 2019. The Pleistocene geoarchaeology and geochronology of con Moong Cave, North Vietnam: site formation processes and hominin activity in the humid tropics. Geoarchaeology 35 (1), 72–97. https://doi.org/10.1002/gea.21758.

Moldovan, O.T., Constantin, S., Panaiotu, C., Roban, R.D., Frenzel, P., Miko, L., 2016. Fossil invertebrates records in cave sediments and paleoenvironmental assessment – a study of four cave sites from Romanian Carpathians. Biogeosciences 13, 483–497. https://doi.org/10.5194/bg-13-483-2016.

Moore, P.D., Webb, J.A., Collinson, M.E., 1991. Pollen analysis, 2nd ed. Blackwell, Oxford, pp. 1–216.

Mullins, C., 1977. Magnetic susceptibility of the soil and its significance in soil science—a review. Eur. J. Soil Sci. 28, 223–246. https://doi.org/10.1111/j.1365-2389.1977.tb02232.x.

Nagavciuc, V., Ionita, M., Kern, Z., et al., 2022. A ~700 years perspective on the 21st century drying in the eastern part of Europe based on $\delta^{18}O$ in tree ring cellulose. Communicat. Earth & Environ. 3, 277. https://doi.org/10.1038/s43247-022-00605-4.

Onac, B.P., Ghergari, L., Gal, A., 1995. Crystallographical studies on gypsum crystals in Ponoraş Cave (Pădurea Craiului Mountains, Romania). Theoret. Appl. Karstol. 8, 63–67.

Onac, B.P., Constantin, S., Lundberg, J., Lauritzen, S.-E., 2002. Isotopic climate record in a Holocene stalagmite from Ursilor Cave (Romania). J. Quat. Sci. 17, 319–327. https://doi.org/10.1002/jqs.685.

Onac, B.P., Forray, F.L., Wynn, J.G., Giurgiu, A.M., 2014. Guano-derived $\delta^{13}C$-based paleo-hydroclimate record from Gaura cu Musca Cave, SW Romania. Environ. Earth Sci. 71, 4061–4069. https://doi.org/10.1007/s12665-013-2789-x.

Onac, B.P., Hutchinson, S., Geantă, A., Forray, F.L., Wynn, J.G., Giurgiu, A., Coroiu, I., 2015. A 2500-yr late Holocene multi-proxy record of vegetation and hydrologic changes from a cave guano-clay sequence in SW Romania. Quat. Res. 83 (3), 437–448. https://doi.org/10.1016/j.yqres.2015.01.007.

Osborne, R.A.L., 1986. Sedimentation in Caves - a Review, vol. 2. Publications of the Geological Society of Australia, pp. 189–217.

Panait, A., Diaconu, A., Galka, M., Grindean, R., Hutchinson, S.M., Hickler, T., Lamentowicz, M., Mulch, A., Tanţău, I., Werner, C., Feurdean, A., 2017. Hydrological conditions and carbon accumulation rates reconstructed from a mountain raised bog in the Carpathians: a multi-proxy approach. Catena 152, 57–68. https://doi.org/10.1016/j.catena.2016.12.023.

Perşoiu, I., Perşoiu, A., 2018. Flood events in Transylvania during the medieval warm period and the Little Ice Age. The Holocene 29 (1), 85–96. https://doi.org/10.1177/0959683618804632.

Perşoiu, A., Onac, B.P., Wynn, J.G., Blaauw, M., Ionita, M., Hansson, M., 2017. Holocene winter climate variability in Central and Eastern Europe. Sci. Rep. 7 (1), 1196. https://doi.org/10.1038/s41598-017-01397-w.

Plotnick, R.E., Kenig, F., Scott, A.C., 2015. Using the voids to fill the gaps: caves, time, and stratigraphy. Geol. Soc. Spec. Publ. 404, 233–250. https://doi.org/10.1144/SP404.5.

Popa, I., Kern, Z., 2009. Long-term summer temperature reconstruction inferred from tree-ring records from the Eastern Carpathians. Clim. Dyn. 32, 1107–1117. https://doi.org/10.1007/s00382-008-0439-x.

R Core Team, 2023. R: A Language and Environment for Statistical Computing. R Foundation for Statistical Computing, Vienna, Austria. URL. https://www.R-project.org/.

Raczky, P., 2014. Settlement in south-East Europe. In: Fowler, C., Harding, J., Hofmann, D. (Eds.), The Oxford Handbook of Neolithic Europe. Oxford University Press, Oxford, pp. 235–254. https://doi.org/10.1093/oxfordhb/9780199545841.013.072.

Ramos-Román, M.J., De Jonge, C., Magyari, E., Veres, D., Ilvonen, L., Develle, A.-L., Seppä, H., 2022. Lipid biomarker (brGDGT)- and pollen-based reconstruction of temperature change during the Middle to late Holocene transition in the Carpathians. Glob. Planet. Chang. 215, 103859. https://doi.org/10.1016/j.gloplacha.2022.103859.

Reimer, P.J., Austin, W.E., Bard, E., Bayliss, A., Blackwell, P.G., Ramsey, C.B., Butzin, M., Cheng, H., Edwards, R.L., Friedrich, M., 2020. The IntCal20 Northern Hemisphere radiocarbon age calibration curve (0–55 cal kBP). Radiocarbon 62 (4), 725–757. https://doi.org/10.1017/RDC.2020.41.

Rusu, T., 1988. Carstul din Munţii Pădurea Craiului. Dacia Cluj-Napoca, p. 254.

Rusu, T., Viehmann, I., Racoviţă, G., Crăciun, V., 1969. Primele urme de paşi ale omului preistoric din peşterile României (First footprints of prehistoric humans from Romanian caves). Ocrotirea Naturii 13, 191–200.

Santisteban, J.I., Mediavilla, R., Lopez-Pamo, E., Dabrio, C.J., Zapata, M.B.R., Garcia, M.J.G., Castano, S., Martinez-Alfaro, P.E., 2004. Loss on ignition: a qualitative or quantitative method for organic matter and carbonate mineral content in sediments? J. Paleolimnol. 32, 287–299. https://doi.org/10.1023/B:JOPL.0000042999.30131.5b.

Sasowsky, I.D., Mylroie, J.E. (Eds.), 2004. Studies of Cave Sediments. Kluwer Academic/Plenum Publisher, New York, p. 329.

Savu, M., Gogâltan, F., 2021. Sondajul arheologic din Peştera Ungurului de la Şuncuiuş (1995). Stud. Histor. Transylvaniensia 3, 30–68.

Shumilovskikh, L., O'Keefe, J.M.K., Marret, F., 2021. An overview of the taxonomic groups of non-pollen palynomorphs, applications of Non-Pollen Palynomorphs: from Palaeoenvironmental Reconstructions to Biostratigraphy. Geol. Soc. London 511, 13–61. https://doi.org/10.1144/sp511-2020-65.

Tanţău, I., Feurdean, A., de Beaulieu, J.L., et al., 2011. Holocene vegetation history in the upper forest belt of the Eastern Romanian Carpathians. Palaeogeogr. Palaeoclimatol. Palaeoecol. 309, 281–290. https://doi.org/10.1016/j.palaeo.2011.06.011.

Toth, M., Magyari, E.K., Buczkó, K., Braun, M., Panagiotopoulos, K., Heiri, O., 2015. Chironomid-inferred Holocene temperature changes in the South Carpathians (Romania). The Holocene 25 (4), 569–582. https://doi.org/10.1177/0959683614565953.

van Geel, B., Buurman, J., Brinkkemper, O., Schelvis, J., Aptroot, A., van Reenen, G., Hakbijl, T., 2003. Environmental reconstruction of a Roman Period settlement site in Uitgeest (the Netherlands), with special reference to coprophilous fungi. J. Archaeol. Sci. 30, 873–883. https://doi.org/10.1016/S0305-4403(02)00265-0.

Wanner, H., Beer, J., Bütikofer, J., Crowley, T., Cubasch, U., Flückiger, J., Goosse, H., Grosjean, M., Joos, F., Kaplan, J., Küttel, M., Müller, S., Prentice, I., Solomina, O., Stocker, T., Tarasov, P., Wagner, M., Widmann, M., 2008. Mid- to late Holocene climate change: an overview. Quat. Sci. Rev. 27, 1791–1828. https://doi.org/10.1016/j.quascirev.2008.06.013.

Warken, S.F., Fohlmeister, J., Schröder-Ritzrau, A., Constantin, S., Spötl, C., Gerdes, A., Esper, J., Frank, N., Arps, J., Terente, M., Riechelmann, D.F.C., Mangini, A., Scholz, D., 2018. Reconstruction of late Holocene autumn/winter precipitation variability in SW Romania from a high-resolution speleothem trace element record. Earth Planet. Sci. Lett. 499, 122–133. https://doi.org/10.1016/j.epsl.2018.07.027.

Webb, D., Robu, M., Moldovan, O., Constantin, S., Tomuş, B., Neag, I., 2014. Ancient human footprints in Ciur Izbuc cave, Romania. Am. J. Phys. Anthropol. 155, 128–135. https://doi.org/10.1002/ajpa.22561.

White, W.B., 2007. Cave sediments and paleoclimate. J. Cave Karst Studies 69, 76–93.

Whitlock, C., Larsen, C., 2001. Charcoal as a fire proxy. In: Smol, J.P., Birks, H.J.B., Last, W.M., Bradley, R.S., Alverson, K. (Eds.), Tracking Environmental Change Using Lake Sediments: Terrestrial, Algal, and Siliceous Indicators. Springer, Dordrecht, pp. 75–97.